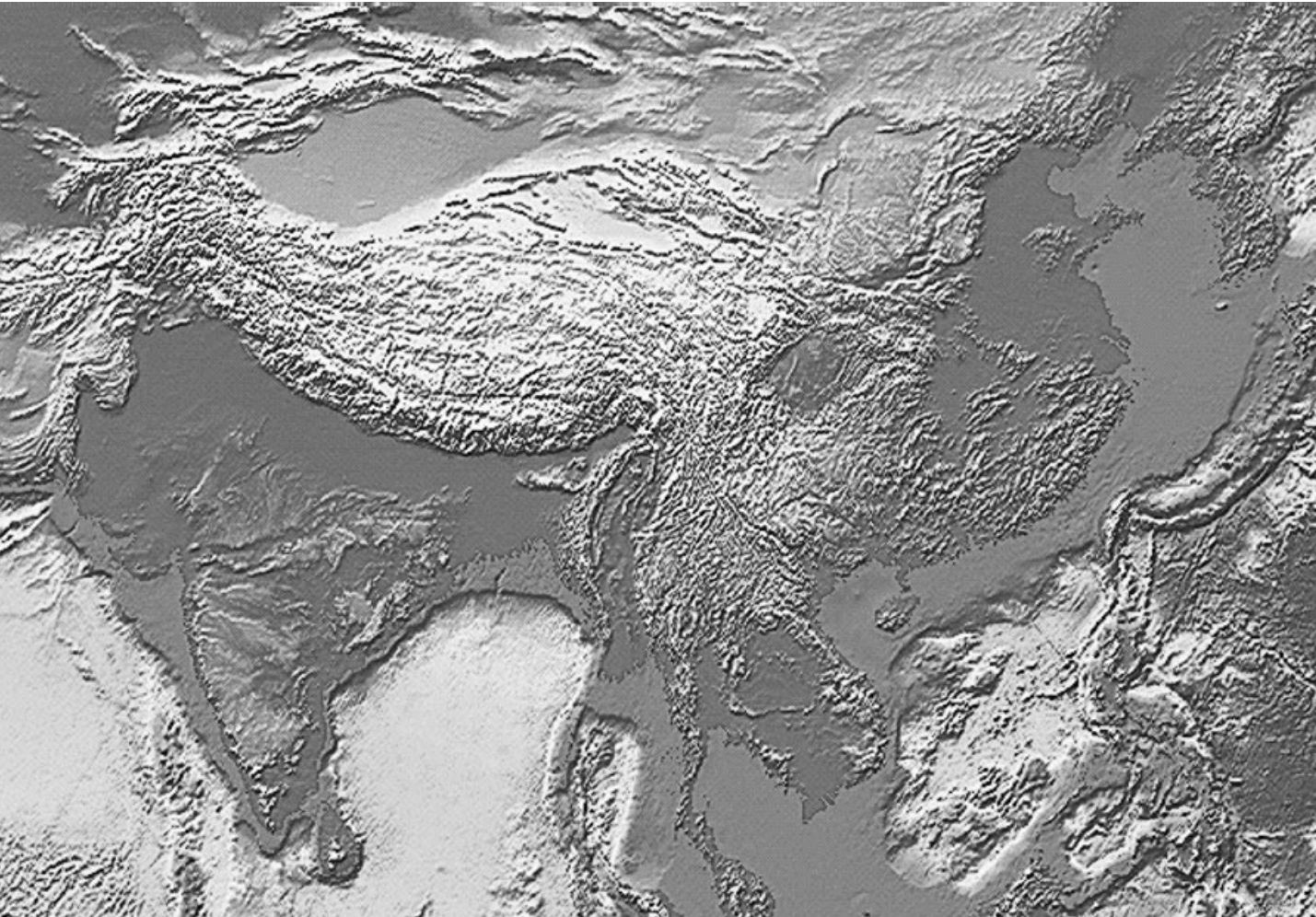


# 6

## Ocean ridges



## 6.1 OCEAN RIDGE TOPOGRAPHY

Ocean ridges mark accretive, or constructive plate margins where new oceanic lithosphere is created. They represent the longest, linear uplifted features of the Earth's surface, and can be traced by a belt of shallow focus earthquakes that follows the crestral regions and transform faults between offset ridge crests (Fig. 5.2). The total length of the spreading margins on mid-ocean ridges is approximately 55,000 km. The total length of the active ridge-ridge transform faults is in excess of 30,000 km. The topographic expression of mid-ocean ridges is typically between 1000 and 4000 km in width. Their crests are commonly 2–3 km higher than neighboring ocean basins, and locally the topography can be quite rugged and runs parallel to the crests.

The gross morphology of ridges appears to be controlled by separation rate (Macdonald, 1982). Spreading rates at different points around the mid-ocean ridge system vary widely. In the Eurasian basin of the Arctic Ocean, and along the Southwest Indian Ocean Ridge, the full spreading rate (the accretion rate) is less than  $20 \text{ mm a}^{-1}$ . On the East Pacific Rise, between the Nazca and Pacific plates, the accretion rate ranges up to  $150 \text{ mm a}^{-1}$ . It is not surprising therefore that many of the essential characteristics of the ridges, such as topography, structure, and rock types, vary as a function of spreading rate. Very early on it was recognized that the

gross topography of the East Pacific Rise, which is relatively smooth, even in the crestral region, contrasts with the rugged topography of the Mid-Atlantic Ridge, which typically has a median rift valley at its crest. This can now be seen to correlate with the systematically different spreading rates on the two ridges (Fig. 5.5), that is, fast and slow respectively. These two types of ridge crest are illustrated in Fig. 6.1, which is based on detailed bathymetric data obtained using deeply towed instrument packages. In each case, the axis of spreading is marked by a narrow zone of volcanic activity that is flanked by zones of fissuring. Away from this volcanic zone, the topography is controlled by vertical tectonics on normal faults. Beyond distances of 10–25 km from the axis, the lithosphere becomes stable and rigid. These stable regions bound the area where oceanic lithosphere is generated – an area known as the “crestral accretion zone” or “plate boundary zone”.

The fault scarps on fast-spreading ridges are tens of meters in height, and an axial topographic high, up to 400 m in height and 1–2 km in width, commonly is present. Within this high a small linear depression, or graben, less than 100 m wide and up to 10 m deep is sometimes developed (Carbotte & Macdonald, 1994). The axial high may be continuous along the ridge crest for tens or even hundreds of kilometers. On slow-spreading ridges the median rift valley is typically 30–50 km wide and 500–2500 m deep, with an inner valley floor, up to 12 km in width, bounded by normal fault scarps approximately 100 m in height. Again there is often an axial topographic high, 1–5 km in width, with hundred of meters of relief, but extending for only tens

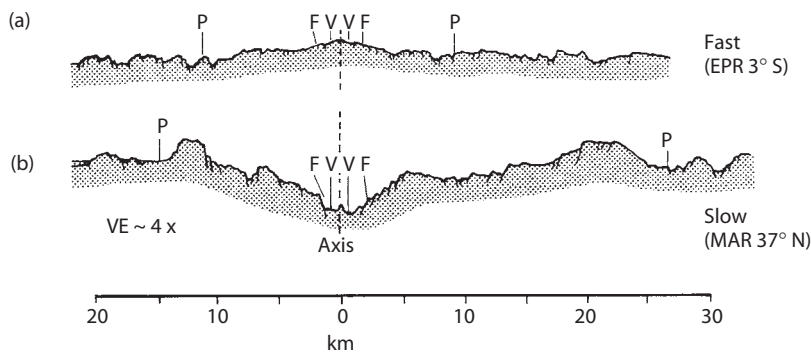


**Fig. 6.1** Bathymetric profiles of ocean ridges at fast and slow spreading rates. EPR, East Pacific Rise; MAR, Mid-Atlantic Ridge. Neovolcanic zone bracketed by Vs, zone of fissuring by Fs, extent of active faulting by Ps (redrawn with permission from MacDonald, 1982, Annual Review of Earth and Planetary Sciences **10**. Copyright © 1982 by Annual Reviews).

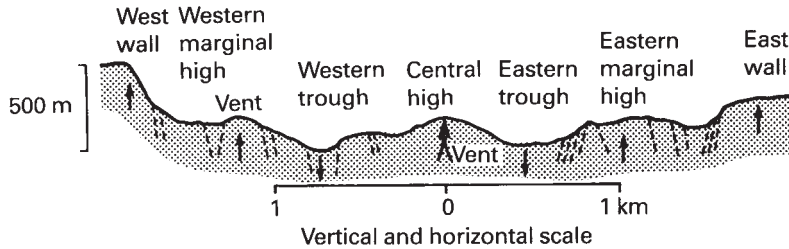


**Fig. 6.2** Diagrammatic cross-section of the inner rift valley of the Mid-Atlantic Ridge at  $36^{\circ}50'N$  in the FAMOUS area (redrawn from Ballard & van Andel, 1977, with permission from the Geological Society of America).

of kilometers along the axis. At fast rates of spreading the high may arise from the buoyancy of hot rock at shallow depth, but on slowly spreading ridges it is clearly formed by the coalescence of small volcanoes 1–2 km in width, and hence is known as an axial volcanic ridge (Smith & Cann, 1993).

A detailed study of a median rift valley was made in the Atlantic Ocean between latitudes  $36^{\circ}30'$  and  $37^{\circ}N$ , a region known as the FAMOUS (Franco-American Mid-Ocean Undersea Study) area, using both surface craft and submersibles (Ballard & van Andel, 1977). The median rift in this area is some 30 km wide, bounded by flanks about 1300 m deep, and reaches depths between 2500 and 2800 m. In some areas the inner rift valley is 1–4 km wide and flanked by a series of fault-controlled terraces (Fig. 6.2). Elsewhere, however, the inner floor is wider with very narrow or no terraces developed. The normal faults that control the terracing and walls of the inner rift are probably the locations where crustal blocks are progressively raised, eventually to become the walls of the rift and thence ocean floor, as they are carried laterally away from the rift by sea floor spreading. Karson *et al.* (1987) described investigations of the Mid-Atlantic Ridge at  $24^{\circ}N$  using a submersible, deep-towed camera and side-scan sonar. Along a portion of the ridge some 80 km long they found considerable changes in the morphology, tectonic activity, and volcanism of the median valley. By incorporating data supplied by investigations of the Mid-Atlantic Ridge elsewhere, they concluded that the development of the style of the median valley may be a cyclic process between phases of tectonic extension and volcanic construction.

Bicknell *et al.* (1988) reported on a detailed survey of the East Pacific Rise at  $19^{\circ}30'S$ . They found that faulting is more prevalent than on slow-spreading ridges, and conclude that faulting accounts for the vast majority of

the relief. They observed both inward and outward facing fault scarps that give rise to a horst and graben topography. This differs from slower spreading ridges, where the topography is formed by back-tilted, inward-facing normal faults. Active faulting is confined to the region within 8 km of the ridge axis, and is asymmetric with the greater intensity on the eastern flank. The half extension rate due to the faulting is  $4.1 \text{ mm a}^{-1}$ , compared to  $1.6 \text{ mm a}^{-1}$  observed on the Mid-Atlantic Ridge in the FAMOUS area.

Historically, for logistical reasons, the slowest spreading ridges, the Southwest Indian Ocean Ridge and the Gakkel Ridge of the Arctic Ocean, were the last to be studied in detail. In the Arctic the year-round ice cover necessitated the use of two research icebreakers (Michael *et al.*, 2003). The results of these studies led Dick *et al.* (2003) to suggest that there are three types of ridge as a function of spreading rate: fast, slow, and ultraslow (Fig. 6.3). Although the topography of the ultraslow Gakkel Ridge is analogous to that of slow-spreading ridges, typically with a well-developed median rift, the distinctive crustal thickness (Fig. 6.3), the lack of transform faults, and the petrology of this ridge set it apart as a separate class. Note that there are two additional categories of ridge with spreading rates between those of fast and slow, and slow and ultraslow, termed intermediate and very slow respectively. Intermediate spreading rate ridges may exhibit the characteristics of slow or fast-spreading ridges, and tend to alternate between the two with time. Similarly, a very slow-spreading ridge may exhibit the characteristics of a slow or ultraslow ridge. It is interesting to note that at the present day the East Pacific Rise is the only example of a fast-spreading ridge and the Gakkel Ridge of the Arctic is the only ultraslow-spreading ridge. Differences between the crustal structure and petrology of fast, slow and ultraslow ridges are discussed in Sections 6.6–6.9.

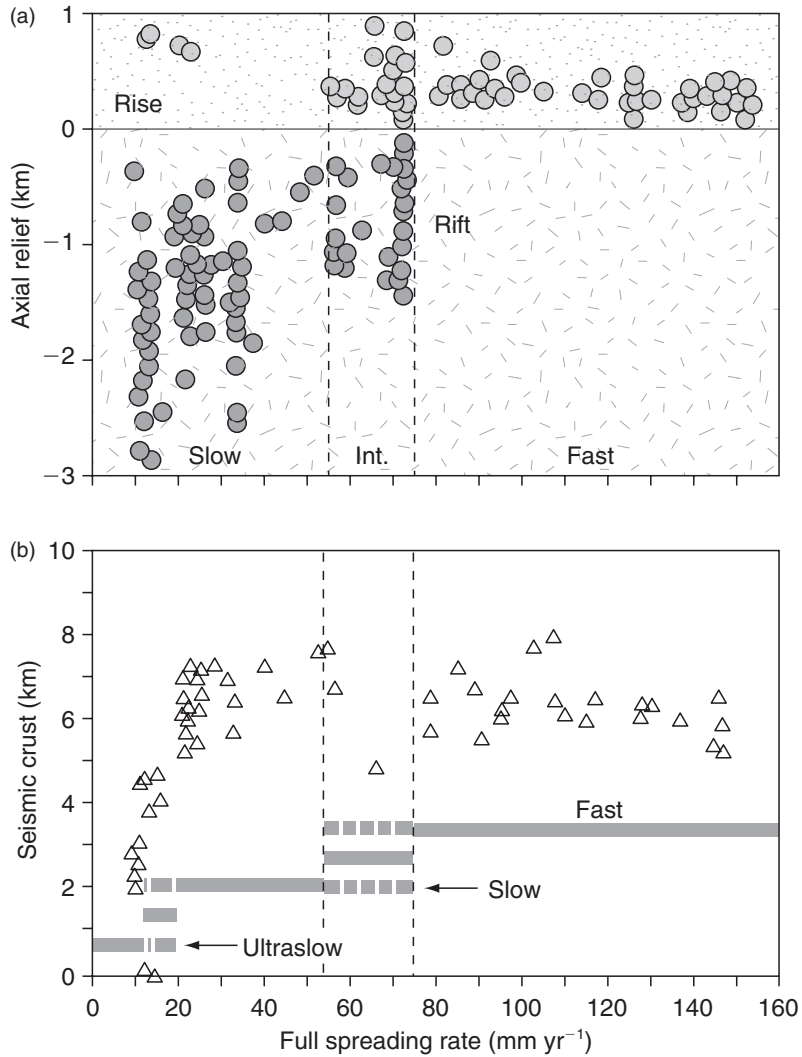


**Fig. 6.3** (a) Axial relief and (b) seismic crustal thickness as a function of full spreading rate at mid-ocean ridge crests. A ridge classification scheme is shown by the heavy black straight lines which indicate the spreading rate ranges for ultraslow, slow, fast and two intermediate classes (modified from Dick et al., 2003, with permission from *Nature* **426**, 405–12. Copyright © 2003 Macmillan Publishers Ltd).

## 6.2 BROAD STRUCTURE OF THE UPPER MANTLE BELOW RIDGES

Gravity measurements have shown that free air anomalies are broadly zero over ridges (Figs 6.4, 6.5), indicating that they are in a state of isostatic equilibrium (Section 2.11.6), although small-scale topographic features are uncompensated and cause positive and negative free air anomalies. The small, long wavelength, positive and negative free air anomalies over the crests and flanks, respectively, of ridges are a consequence of the compensation, with the positives being caused by the greater elevation of the ridge and the negatives from the compensating mass deficiency. The gravitational effects of the compensation dominate the gravity field away from the ridge crest, and indicate that the compensation is deep.

Seismic refraction experiments by Talwani *et al.* (1965) over the East Pacific Rise showed that the crust

is slightly thinner than encountered in the main ocean basins, and that the upper mantle velocity beneath the crestral region is anomalously low (Fig. 6.4). Oceanic layer 1 rocks (Section 2.4.5) are only present within topographic depressions, but layers 2 and 3 appear to be continuous across the ridge except for a narrow region at the crest. A similar structure has been determined for the Mid-Atlantic Ridge (Fig. 6.5). The suggestion of this latter work that layer 3 is not continuous across the ridge was subsequently disproved (Whitmarsh, 1975; Fowler, 1976).

As the crust does not thicken beneath ridges, isostatic compensation must occur within the upper mantle by a Pratt-type mechanism (Section 2.11.3). Talwani *et al.* (1965) proposed that the anomalously low upper mantle velocities detected beneath ridges correspond to the tops of regions of low density. The densities were determined by making use of the Nafe–Drake relationship between P wave velocity and density (Nafe & Drake, 1963), and a series of models produced that satisfied both the seismic and gravity data. One of these is shown in Fig. 6.6, and indicates the presence beneath the ridge of a body with a density contrast of  $-0.25 \text{ Mg m}^{-3}$  extending to a depth of some 30 km. This large density contrast is difficult to explain geologically. An alternative interpretation, constructed by Keen & Tramontini (1970), is shown in Fig. 6.7. A much lower,

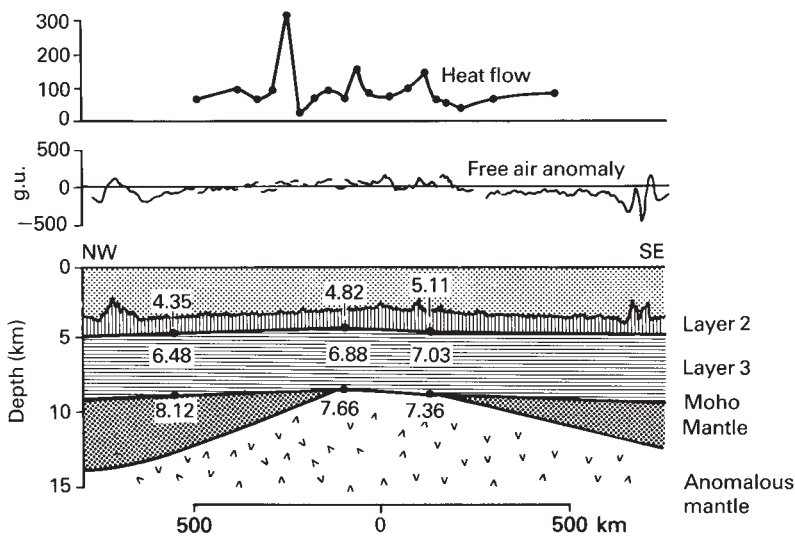


**Fig. 6.4** Heat flow, free air gravity anomaly and crustal structure defined by seismic refraction across the East Pacific Rise at 15–17°S. P wave velocities in  $\text{km s}^{-1}$  (redrawn from Talwani *et al.*, 1965, by permission of the American Geophysical Union. Copyright © 1965 American Geophysical Union).

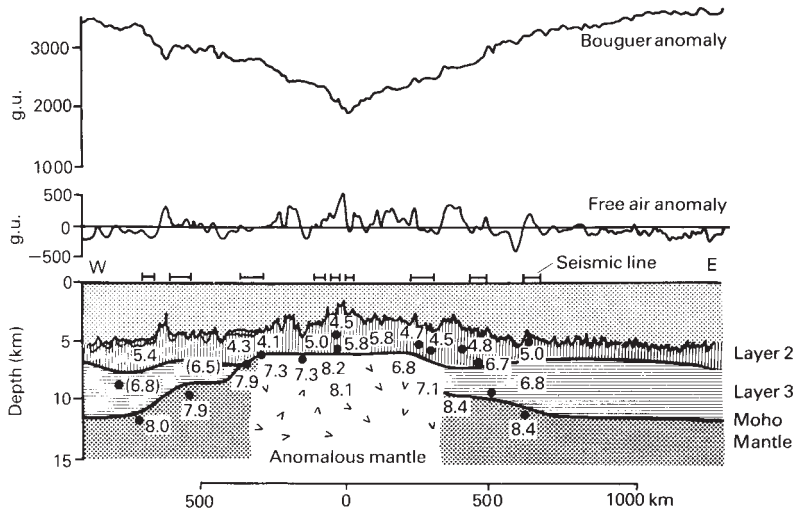


**Fig. 6.5** Gravity anomalies and crustal structure defined by seismic refraction across the Mid-Atlantic Ridge at about  $31^{\circ}\text{N}$ . Bouguer anomaly reduction density  $2.60\text{ Mg m}^{-3}$ , P wave velocities in  $\text{km s}^{-1}$  (redrawn from Talwani et al., 1965, by permission of the American Geophysical Union. Copyright © 1965 American Geophysical Union).

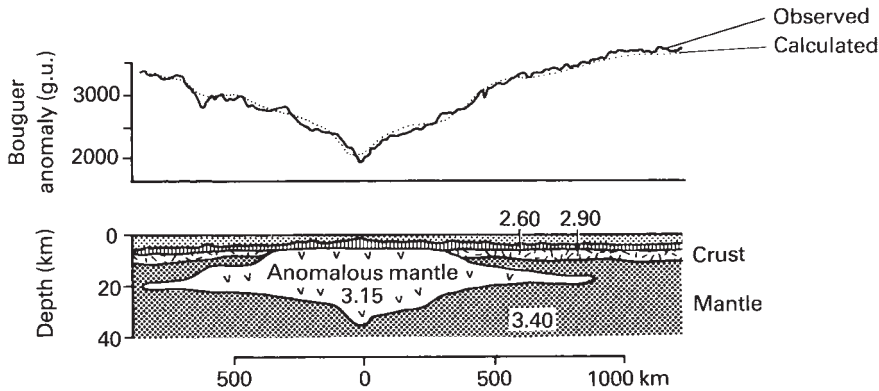


**Fig. 6.6** Possible model of the structure beneath the Mid-Atlantic Ridge from gravity modeling with seismic refraction control. Densities in  $\text{Mg m}^{-3}$  (redrawn from Talwani et al., 1965, by permission of the American Geophysical Union. Copyright © 1965 American Geophysical Union).

more realistic density contrast of  $-0.04\text{ Mg m}^{-3}$  is employed, and the anomalous body is considerably larger, extending to a depth of 200 km. However, this model can also be criticized in that the densities employed are rather too high, and provide too low a density contrast, and the depth to the base of the anomalous mass is too great. A model that employs densities of  $3.35$  and  $3.28\text{ Mg m}^{-3}$  for normal and anomalous

mantle, respectively, with the anomalous mass extending to a depth of 100 km, would be more in accord with geologic and geophysical data. Indeed, seismic tomography (Section 2.1.8) suggests that the low velocity region beneath ocean ridges extends to a depth of 100 km (Anderson et al., 1992).

Given the ambiguity inherent in gravity modeling, the two interpretations shown probably represent end

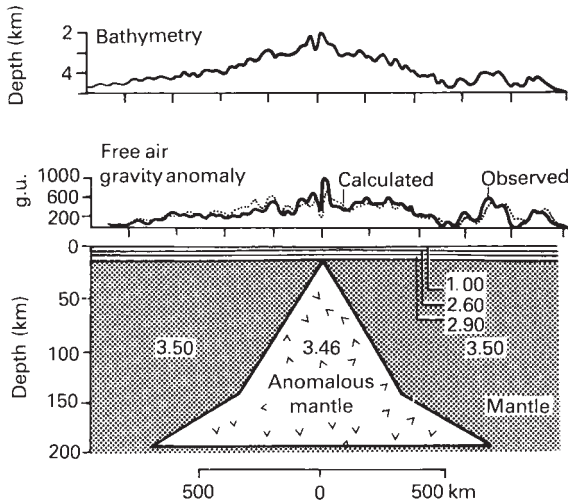


**Fig. 6.7** Alternative model of the structure beneath the Mid-Atlantic Ridge from gravity modeling. Profile at 46°N. Densities in  $\text{Mg m}^{-3}$  (redrawn from Keen & Tramontini, 1970, with permission from Blackwell Publishing).

members of a suite of possible interpretations. They demonstrate without ambiguity, however, that ridges are underlain by large, low-density bodies in the upper mantle whose upper surfaces slope away from the ridge crests.

## 6.3 ORIGIN OF ANOMALOUS UPPER MANTLE BENEATH RIDGES

There are three possible sources of the low-density regions which underlie ocean ridges and support them isostatically (Bott, 1982): (i) thermal expansion of upper mantle material beneath the ridge crests, followed by contraction as sea floor spreading carries it laterally away from the source of heat, (ii) the presence of molten material within the anomalous mantle,

(iii) a temperature-dependent phase change. The high temperatures beneath ocean ridge crests might cause a transition to a mineralogy of lower density.

Suppose the average temperature to a depth of 100 km below the Moho is 500°C greater at the ridge crest than beneath the flanking regions, the average density to this depth is  $3.3 \text{ Mg m}^{-3}$  and the volume coefficient of thermal expansion is  $3 \times 10^{-5}$  per degree. In this case the average mantle density to a depth of 100 km would be  $0.05 \text{ Mg m}^{-3}$  less than that of the flanking ocean basins. If isostatic equilibrium were attained, this low-density region would support a ridge elevated 2.2 km above the flanking areas. If the degree of partial melting were 1%, the consequent decrease in density would be about  $0.006 \text{ Mg m}^{-3}$ . Extended over a depth range of 100 km this density contrast would support a relative ridge elevation of 0.25 km. The aluminous minerals within the upper mantle that might transform to a lower density phase are also the minerals that enter the melt that forms beneath the ridge crest. They are absent therefore in the bulk of the mantle volume under consideration, which consists of depleted mantle; mantle from which the lowest melting point fraction has been removed. It is unlikely then that a phase change contributes significantly to the uplift.

Partial melting of the upper mantle clearly is a reality because of the magmatic activity at ridge crests, but its extent was a matter of conjecture. However, in the mid-1990s a very large-scale experiment, the Mantle Electromagnetic and Tomography (MELT) experiment, was carried out on the crest of the East Pacific Rise specifically to define the vertical and lateral extent of the region of partial melting beneath it (MELT seismic team, 1998). Fifty-one ocean bottom seismometers and 47 instruments that measure changes in the Earth's magnetic and electric fields were deployed across the ridge, between 15° and 18°S, in two linear arrays each approximately 800 km long. This location was chosen because it is in the middle of a long, straight section of the ridge between the Nazca and Pacific plates, and has one of the fastest spreading rates:  $146 \text{ mm a}^{-1}$  at 17°S. The extent of any partial melt in the mantle should therefore be well developed in terms of low seismic velocities and high electrical conductivity. Seismic waves from regional and teleseismic earthquakes, and variations in the Earth's electric and magnetic fields, were recorded for a period of approximately 6 months. Analysis of the data revealed an asymmetric region of low seismic velocities extending to a depth of 100 km, with

its shallowest point beneath the ridge crest, but extending to 350 km to the west and 150 km to the east of the ridge crest (Fig. 6.8). Both the velocity anomalies and electrical conductivity are consistent with 1–2% partial melting (Evans *et al.*, 1999). There is an indication of incipient melting to a depth of 180 km. The asymmetry of the region of partial melting is thought to be due to a combination of two effects. Within the hot spot framework the western flank of the ridge is moving at more than twice the rate of the eastern flank (Fig. 6.8). It is also close to the South Pacific superswell (Section 12.8.3). Enhanced upwelling and hence flow in the asthenosphere from the superswell and viscous drag beneath the fast moving Pacific plate are thought to produce higher rates of flow and hence higher temperatures beneath the western flank of the ridge. These elevated temperatures are reflected in shallower bathymetry (Section 6.4) and a higher density of seamount volcanism on the western flank compared to the eastern flank.

The width of the region of partial melt defined by the MELT experiment seems to be quite wide. One must recall however that the spreading rate at this point is very high, five times higher than that on much

of the Mid-Atlantic Ridge. In fact the region of primary melt only underlies crust 2–3 Ma in age, whereas the anomalous uplift of ridges extends out to crust of 70–80 Ma in age. Partial melt in the upper mantle may therefore account for some of the uplift of ridge crests but cannot account for the uplift of ridge flanks.

## 6.4 DEPTH-AGE RELATIONSHIP OF OCEANIC LITHOSPHERE

The major factor contributing to the uplift of mid-ocean ridges is the expansion and contraction of the material of the upper mantle. As newly formed oceanic lithosphere moves away from a mid-ocean

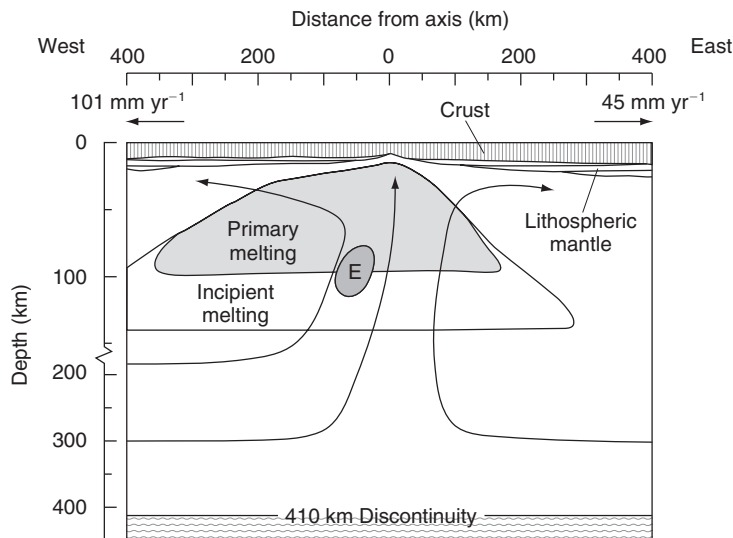


**Fig. 6.8** Schematic cross-section beneath the East Pacific Rise at 17°S illustrating the extent of partial melting in the mantle deduced from the results of the MELT experiment. Plate velocities are in the hot spot reference frame. The region labeled E (embedded heterogeneity) indicates enhanced melting due to anomalously enriched mantle or localized upwelling (modified from MELT seismic team, 1998, *Science* **280**, 1215–18, with permission from the AAAS).



ridge, it becomes removed from underlying heat sources and cools. This cooling has two effects. First, the lithosphere contracts and increases in density. Second, because the lithosphere–asthenosphere boundary is controlled by temperature (Section 2.12), the cooling causes the lithosphere to increase in thickness away from the mid-ocean ridge. This latter phenomenon has been confirmed by lithosphere thickness estimates derived from surface wave dispersion studies in the Pacific Ocean, which indicate that the thickness increases from only a few kilometers at the ridge crest to 30 km at 5 Ma age and 100 km at 50 Ma (Forsyth, 1977).

The cooling and contraction of the lithosphere cause a progressive increase in the depth to the top of the lithosphere away from the ridge (Sclater & Francheteau, 1970), accompanied by a decrease in heat flow. It follows that the width of a ridge depends upon the spreading rate, and so provides an explanation for the relative widths of the rapidly spreading East Pacific Rise and more slowly spreading Mid-Atlantic Ridge. Parsons & Sclater (1977) determined the nature of the age–depth relationships of oceanic lithosphere, and suggested that the depth  $d$  (meters) is related to age  $t$  (Ma) by:

$$d = 2500 + 350t^{1/2}$$

It was found, however, that this relationship only holds for oceanic lithosphere younger than 70 Ma. For older lithosphere the relationship indicates a more gradual increase of depth with age. In order to explain this, Parsons & McKenzie (1978) suggested a model in which the cooling layer comprises two units rather than the single unit implied by Parsons & Sclater (1977). In this model the upper unit, through which heat moves by conduction, is mechanically rigid, and the lower unit is a viscous thermal boundary layer. As the lithosphere travels away from a spreading center, both units thicken and provide the relationship – depth proportional to the square root of age – described above. However, the lower unit eventually thickens to the point at which it becomes unstable and starts to convect. This brings extra heat to the base of the upper layer and prevents it thickening at the same rate. They suggested that the age–depth relationship for oceanic lithosphere older than 70 Ma is then given by:

$$d = 6400 - 3200\exp(-t/62.8)$$

These two models, for the cooling and contraction of oceanic lithosphere with age, are referred to as the half space and plate models respectively. In the former the lithosphere cools indefinitely, whereas in the latter it ultimately attains an equilibrium situation determined by the temperature at the lithosphere–asthenosphere boundary and the depth at which this occurs as a result of convection in the asthenosphere. Clearly the main constraints on these models are the observed depth (corrected for sediment loading) and heat flux at the ocean floor as a function of age. Stein & Stein (1992), using a large global data set of depth and heat flow measurements, derived a model (GDH1 – global depth and heat flow model 1) that gave the best fit to the observations. Any such model must make assumptions about the depth to the ridge crest and the thermal expansion coefficient, the thermal conductivity, the specific heat, and the density of the lithosphere. However Stein & Stein (1992) showed that the crucial parameters in determining the best fit to the data are the limiting plate thickness and the temperature at the base of the lithospheric plate. In the GDH1 model these have the values 95 km and 1450°C respectively.

A comparison of the age–depth relationship predicted by the half space model, the Parsons, Sclater & McKenzie model and GDH1, is shown in Fig. 6.9a and the depth–age equations for GDH1 are:

$$d = 2600 + 365t^{1/2} \quad \text{for } t < 20 \text{ Ma}$$

$$\text{and } d = 5650 - 2473\exp(-t/36) \quad \text{for } t > 20 \text{ Ma.}$$

## 6.5 HEAT FLOW AND HYDROTHERMAL CIRCULATION

The half space model of lithospheric cooling with age predicts that the heat flux through the ocean floor on ridge flanks will vary in proportion to the inverse square root of its age, but across older ocean floor measured heat flow values vary more slowly than this, again favoring a plate model. The GDH1 model of Stein & Stein (1992) predicts the following values for heat flow,  $q$  ( $\text{mWm}^{-2}$ ) as a function of age,  $t$  (Ma):

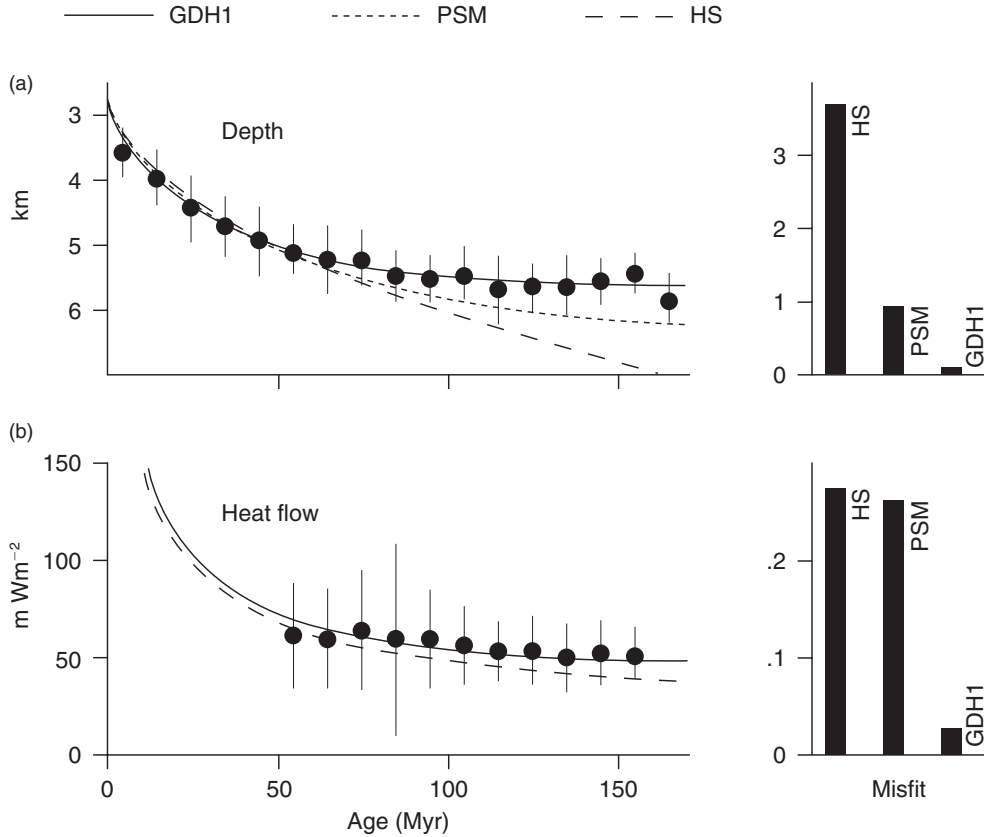


**Fig. 6.9** Observed depth and heat flow data for oceanic ridges plotted as a function of lithospheric age, and compared to the predictions of three thermal models: HS, half space model; PSM, model of Parsons, Sclater and McKenzie; GDH1, global depth and heat flow model of Stein and Stein (redrawn from Stein & Stein, 1996, by permission of American Geophysical Union. Copyright © 1996 American Geophysical Union).

$$q = 510t^{-1/2} \quad \text{for } t \leq 55 \text{ Ma}$$

$$\text{and } q = 48 + 96\exp(-t/36) \quad \text{for } t > 55 \text{ Ma.}$$

The variation of heat flow with age predicted by all three thermal models is illustrated in Fig. 6.9b and compared to observed heat flow values. It will be noted that observed values for younger lithosphere have not been plotted. This is because there are large variations in the heat flux measured in young oceanic crust (Fig. 6.4). The values obtained are typically less than those predicted by the models and there is now thought to be good reason for this. In particular, there is a large scatter in heat flow magnitude near the crests of ocean ridges. Thermal lows tend to occur in flat-floored valleys and highs within areas of rugged topography (Lister, 1980).

Blanketing by sediment does not appear to be the cause of the low heat flow because the troughs are within the least sedimented areas of the ridge and also the youngest and therefore hottest. To explain these phenomena it was proposed that the pattern of heat flow is controlled by the circulation of seawater through the rocks of the oceanic crust.

Although the penetration of water through the hard rock of the sea floor at first seems unlikely, it has been shown that thermal contraction can induce sufficient permeability for efficient convective flow to exist. The cracks are predicted to advance rapidly and cool a large volume of rock in a relatively short time, so that intense localized sources of heat are produced at the surface. Active geothermal systems that are driven by water

coming into contact with near-molten material are expected to be short-lived, but the relatively gentle circulation of cool water, driven by heat conducted from below, should persist for some time. However, as the oceanic crust moves away from the ridge crest, and subsides, it is blanketed by impermeable sediments, and the pores and cracks within it become clogged with minerals deposited from the circulating water. Ultimately heat flux through it is by conduction alone and hence normal heat flow measurements are obtained. This “sealing age” of oceanic crust would appear to be approximately 60 Ma.

Detailed heat flow surveys on the Galapagos Rift revealed that the pattern of large-scale zoning and the wide range of individual values are consistent with hydrothermal circulation (Williams *et al.*, 1974). Small-scale variations are believed to arise from variations in the near-surface permeability, while larger-scale variations are due to major convection patterns which exist in a permeable layer several kilometers thick which is influenced by topography, local venting, and recharge at basement outcrops. The penetration of this convection is not known, but it is possible that it is crust-wide. It is thought that hydrothermal circulation of seawater in the crust beneath ocean ridges transports about 25% of the global heat loss, and is clearly a major factor in the Earth’s thermal budget (Section 2.13).

The prediction of hydrothermal circulation on mid-ocean ridges, to explain the heat flow values observed, was dramatically confirmed by detailed investigations at and near the sea floor at ridge crests, most notably by submersibles. Numerous hydrothermal vent fields have been discovered on both the East Pacific Rise and the Mid-Atlantic Ridge, many of them revealed by the associated exotic and previously unknown forms of life that survive without oxygen or light. The physical and chemical properties of the venting fluids and the remarkable microbial and macrofaunal communities associated with these vents, have been reviewed by Kelly *et al.* (2002). The temperature of the venting fluids can, exceptionally, be as high as 400°C. The chemistry of the hydrothermal springs on the East Pacific Rise and Mid-Atlantic Ridge is remarkably similar, in spite of the great difference in spreading rates, and suggests that they have equilibrated with a greenschist assemblage of minerals (Campbell *et al.*, 1988). Surprisingly perhaps, because of the cooler environment at the ridge crest, there are high levels of hydrothermal activity at certain locations on the very slow- and ultraslow-spreading Gakkal Ridge. This appears to result from the focusing

of magmatic activity at these points, producing higher temperatures at shallow depths (Michael *et al.*, 2003).

Further evidence that hydrothermal circulation occurs comes from the presence of metalliferous deposits at ridge crests. The metals are those known to be hydrothermally mobile, and must have been leached from the oceanic crust by the ingress of seawater which permitted their extraction in a hot, acidic, sulfide-rich solution (Rona, 1984). On coming into contact with cold seawater on or just below the sea floor the solutions precipitate base metal sulfide deposits. The presence of such deposits is corroborated by studies of ophiolites (Section 13.2.2).

## 6.6 SEISMIC EVIDENCE FOR AN AXIAL MAGMA CHAMBER

---

Models for the formation of oceanic lithosphere normally require a magma chamber beneath the ridge axis from which magma erupts and intrudes to form the lava flows and dikes of layer 2. Solidification of magma within the chamber is thought to lead to the formation of most of oceanic layer 3 (Section 6.10). Evidence for the presence of such a magma chamber has been sought from detailed seismic surveys at ridge crests employing refraction, reflection, and tomographic techniques.

On the fast-spreading East Pacific Rise many of the surveys have been carried out in the area north of the Siqueros Fracture Zone between 8° and 13°N. The area centered on the ridge crest at 9°30′N has been particularly intensively studied (e.g. Herron *et al.*, 1980; Detrick *et al.*, 1987; Vera *et al.*, 1990). More recently additional experiments have been carried out at 14°15′S, on one of the fastest spreading sections of the ridge (Detrick *et al.*, 1993a; Kent *et al.*, 1994). All of these studies have revealed a region of low seismic velocities in the lower crust, 4–8 km wide, and evidence for the top of a magma chamber at varying depths, but typically 1–2 km below the sea floor. There is some indication that the depth to the magma chamber is systematically less at 14°S compared to 9°N on the East

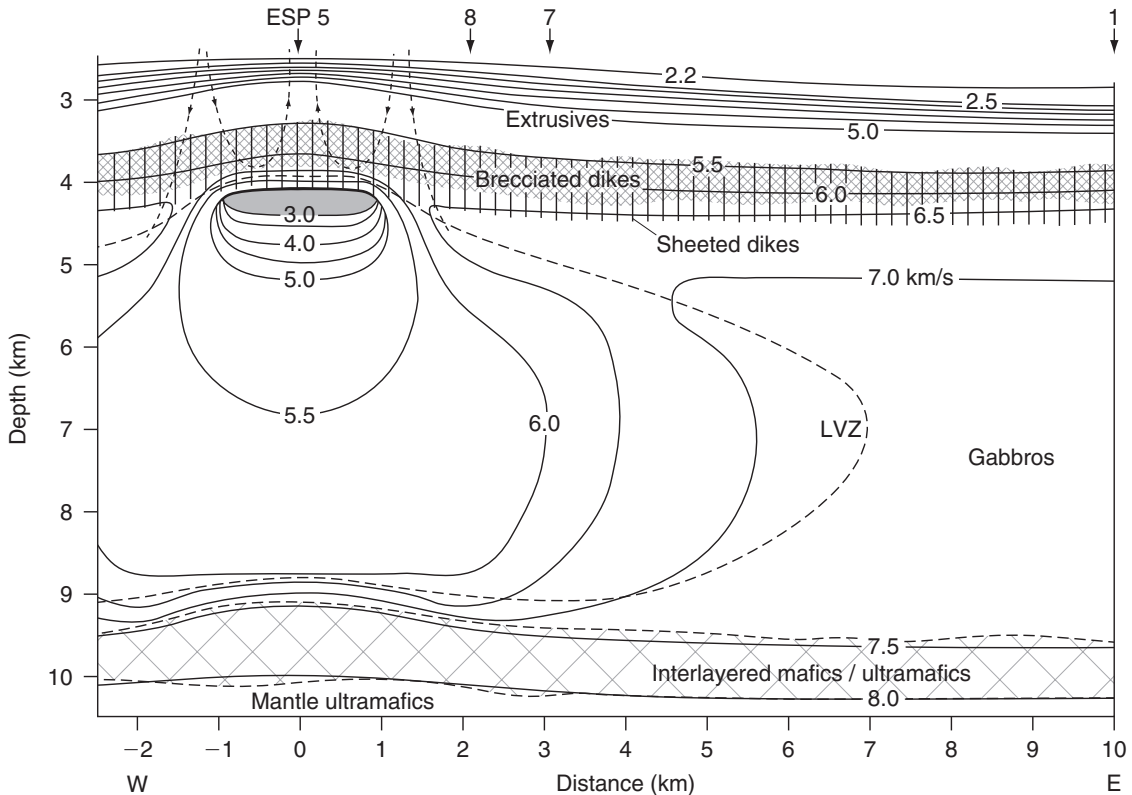


**Fig. 6.10** The variation of P wave velocity in the oceanic crust, at the crest of the East Pacific Rise at  $9^{\circ}30'N$ , deduced from expanded spread (ESP) and common depth point seismic profiling. Shaded area indicates a region with a high percentage of melt. An interpretation of the velocities in terms of rock units, and an indication of the extent of the zone of anomalously low seismic velocities (LVZ), are also shown (redrawn from Vera *et al.*, 1990, by permission of the American Geophysical Union. Copyright © 1990 American Geophysical Union).

Pacific Rise, suggesting an inverse correlation between magma chamber depth and spreading rate (Detrick *et al.*, 1993b). The interpretation of Vera *et al.* (1990) of results obtained at  $9^{\circ}30'N$ , using multi-channel, expanded spread reflection profiling, is shown in Fig. 6.10. They considered that only the volume in which the P-wave velocity is less than  $3 \text{ km s}^{-1}$  can be regarded as a melt lens, and that the region in which the P-wave velocity is greater than  $5 \text{ km s}^{-1}$ , which includes much of the low velocity zone, behaves as a solid. Detrick *et al.* (1987) demonstrated that a strong reflector, thought to be associated with the top of the magma chamber, can be traced as a nearly continuous feature for tens of kilometers along the ridge axis. Much of the

more recent work, typically employing tomographic techniques (Section 2.1.8), suggests that the region in which there is a high melt fraction, probably no more than 30% crystals so that the shear wave velocity is zero, is remarkably small, perhaps no more than a few tens of meters thick, and less than 1 km wide (Kent *et al.*, 1990, 1994; Caress *et al.*, 1992; Detrick *et al.*, 1993a; Collier & Singh, 1997). Thus most of the low velocity zone beneath the ridge crest behaves as a solid and is interpreted as a region of anomalously hot rock.

In contrast to the picture that has emerged for the East Pacific Rise, most seismic studies of the slowly spreading Mid-Atlantic Ridge recognize a low velocity zone in the lower crust beneath the ridge crest but have

not yielded any convincing evidence for a magma chamber or melt lens (Whitmarsh, 1975; Fowler, 1976; Purdy & Detrick, 1986; Detrick *et al.*, 1990). However, Calvert (1995), in reanalyzing the data of Detrick *et al.* (1990) acquired at  $23^{\circ}17'N$ , isolated reflections from a presumed magma chamber at a depth of 1.2 km and with a width of 4 km.

It seems unlikely therefore that steady state magma chambers exist beneath the axes of slowly spreading ridges. Transient magma chambers, however, related to influxes of magma from the mantle, may exist for short periods. In order to test this hypothesis a very detailed combined seismic and electromagnetic experiment was carried out across the Reykjanes Ridge south of Iceland (Sinha *et al.*, 1998). This study was deliberately centered on a magmatically active axial volcanic ridge (AVR) on the Reykjanes Ridge at  $57^{\circ}45'N$ , and did reveal a melt lens and crystal mush zone analogous to those imaged on the East Pacific Rise. In this instance the melt lens occurs at a depth 2.5 km beneath the sea floor. The results of this study provide strong support for the hypothesis that the process of crustal accretion on slow-spreading ridges is analogous to that at fast-spreading ridges but that the magma chambers involved are short-lived rather than steady state. Despite its proximity to the Iceland hot spot, the ridge crest south of  $58^{\circ}N$  on the Reykjanes Ridge has the characteristics of a typical slow-spreading ridge: a median valley, and normal crustal thickness and depth.

The logistically complicated seismic experiments required to test for the presence or absence of a melt lens have yet to be carried out on the very slow- and ultraslow-spreading Gakkal Ridge. It seems extremely unlikely that melt lenses exist beneath the amagmatic segments of this ridge, in that these consist of mantle peridotite with only a thin carapace of basalts, but possible that transient melt lenses occur beneath the magmatic segments and volcanic centers (Section 6.9). However, in 1999 seismological and ship-borne sonar observations recorded a long-lived magmatic-spreading event on the Gakkal Ridge that had characteristics more consistent with the magma being derived directly from mantle depths than from a crustal magma chamber (Tolstoy *et al.*, 2001).

Sinton & Detrick (1992), taking account of the seismic data available at that time and incorporating new ideas on magma chamber processes, proposed a model in which the magma chambers comprise narrow, hot, crystal-melt mush zones. In this model magma chambers are viewed as composite structures compris-

ing an outer transition zone made up of a hot, mostly solidified crust with small amounts of interstitial melts and an inner zone of crystal mush with sufficient melt for it to behave as a very viscous fluid. A melt lens only develops in fast-spreading ridges where there is a sufficiently high rate of magma supply for it to persist at the top of the mush zone (Fig. 6.11a). This lens may extend for tens of kilometers along the ridge crest, but is only 1–2 km wide and tens or hundreds of meters in thickness. Slow-spreading ridges are assumed to have an insufficient rate of magma supply for a melt lens to develop (Fig. 6.11b) and that eruptions only occur when there are periodic influxes of magma from the mantle. Such a model is consistent with the seismic data from ocean ridges and petrologic observations which require magma to have been modified by fractionation within the crust, which could not occur in a large, well-mixed chamber. It also explains why less fractionation occurs in the volcanic rocks of slow-spreading ridges. A problem with this model, however, is that it is not apparent how the layered gabbros of layer 3 might develop.

Subsequent work by Singh *et al.* (1998), involving further processing of the seismic reflection data obtained by Detrick *et al.* (1993a) near to  $14^{\circ}S$  on the East Pacific Rise, was specifically targeted at identifying any along-axis variations in the seismic properties and thickness of the melt lens. Their results suggest that only short, 2–4 km lengths of the melt lens contain pure melt capable of erupting to form the upper crust. The intervening sections of the melt lens, 15–20 km in length, are rich in crystal mush and are assumed to contribute to the formation of the lower crust. It seems probable that the pockets of pure melt are related to the most recent injections of magma from the mantle.

## 6.7 ALONG-AXIS SEGMENTATION OF OCEANIC RIDGES

---

Many early investigations of ocean ridges were essentially two-dimensional in that they were based on quite widely spaced profiles oriented perpendicular to their strike. More recently “swath”-mapping systems have

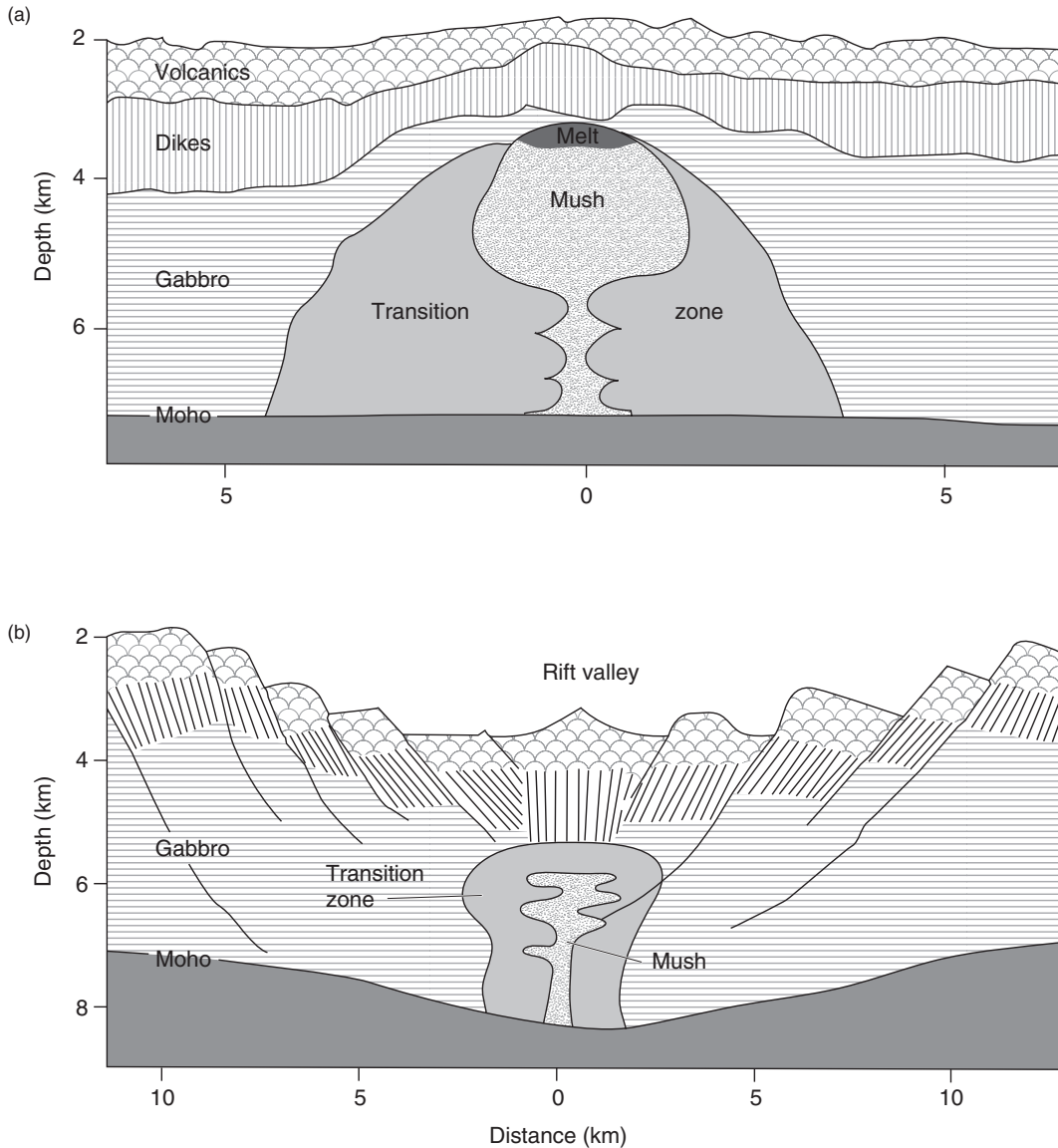


**Fig. 6.11** Interpretive models of magma chambers beneath a fast (a) and slow (b) spreading ridge (modified from Sinton & Detrick, 1992, by permission of the American Geophysical Union. Copyright © 1992 American Geophysical Union).

been employed which provide complete areal coverage of oceanic features. These systems have been used to reveal variations in the structure of ocean ridges along strike. A review of these developments was provided by Macdonald *et al.* (1988).

Studies of the East Pacific Rise have shown that it is segmented along its strike by nontransform ridge axis discontinuities such as propagating rifts (Section 6.11) and overlapping spreading centers (OSC), which occur at local depth maxima, and by smooth variations in the

depth of the ridge axis. These features may migrate up or down the ridge axis with time.

OSCs (MacDonald & Fox, 1983) are nonrigid discontinuities where the spreading center of a ridge is offset by a distance of 0.5–10 km, with the two ridge portions overlapping each other by about three times the offset. It has been proposed that OSCs originate on fast-spreading ridges where lateral offsets are less than 15 km, and true transform faults fail to develop because the lithosphere is too thin and weak. The OSC geometry is obviously unstable, and its development has been deduced from the behavior of slits in a solid wax film floating on molten wax, which appears to represent a reasonable analogue (Fig. 6.12a). Tension applied orthogonal to the slits (spreading centers) causes their lateral propagation (Fig. 6.12b) until they overlap (Fig. 6.12c), and the enclosed zone is subjected to shear and rotational deformation. The OSCs continue to advance until one tip links with the other OSC (Fig. 6.12d). A single spreading center then develops as one OSC becomes inactive and is moved away as spreading continues (Fig. 6.12e).

Fast-spreading ridges are segmented at several different scales (Fig. 6.13). First order segmentation is defined by fracture zones (Section 4.2) and propagating rifts (Section 6.11), which divide the ridge at intervals of 300–500 km by large axial depth anomalies. Second order segmentation at intervals of 50–300 km is caused by nonrigid transform faults (which affect crust that is still thin and hot) and large offset (3–10 km) OSCs that cause axial depth anomalies of hundreds of meters. Third order segmentation at intervals of 30–100 km is defined by small offset (0.5–3 km) OSCs, where depth anomalies are only a few tens of meters. Finally, fourth order segmentation at intervals of 10–50 km is caused by very small lateral offsets (<0.5 km) of the axial rift and small deviations from axial linearity of the ridge axis (DEVALS). These are rarely associated with depth anomalies and may be represented by gaps in the volcanic activity within the central rift or by geochemical variation. Clearly fourth order segmentation is on the same along-axis length scale as the intervals between pure melt pockets in the melt lens documented by Singh *et al.* (1998) (Section 6.6).

Third and fourth order segmentations appear to be short-lived, as their effects can only be traced for a few kilometers in the spreading direction. Second order segmentations, however, create off axis scars on the spreading crust consisting of cusped ridges and elongate basins that cause differential relief of several hundred

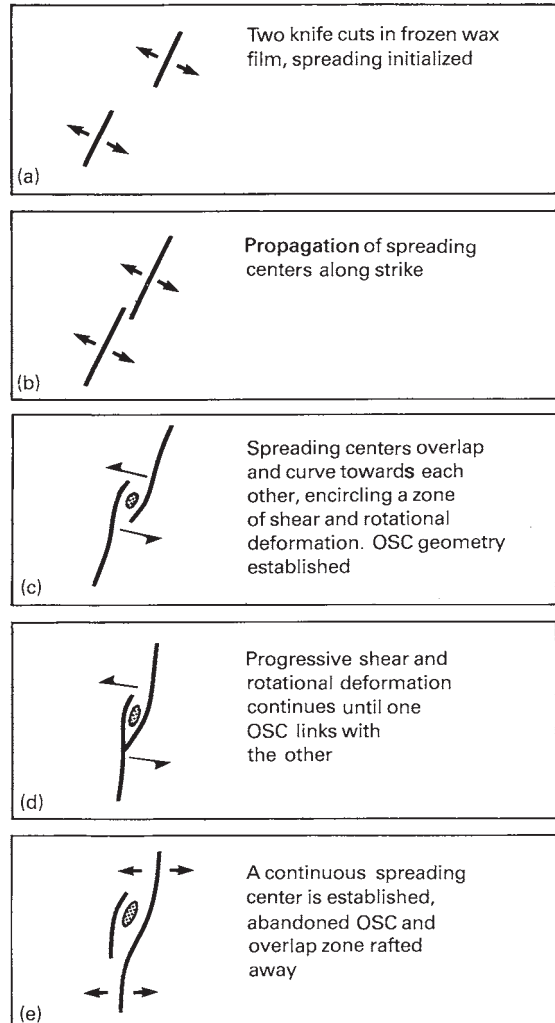


**Fig. 6.12** Possible evolutionary sequence in the development of an overlapping spreading center (redrawn from MacDonald & Fox, 1983, with permission from *Nature* **302**, 55–8. Copyright © 1983 Macmillan Publishers Ltd).

meters. The scars do not follow small circle routes about the spreading pole, but form V-shaped wakes at 60–80° to the ridge. This indicates that the OSCs responsible for the segmentation migrate along the ridge at velocities of up to several hundred millimeters per year. Figure 6.14 summarizes the three general cases for the evolution of such ridge-axis discontinuities in terms of the movement of magma pulses.

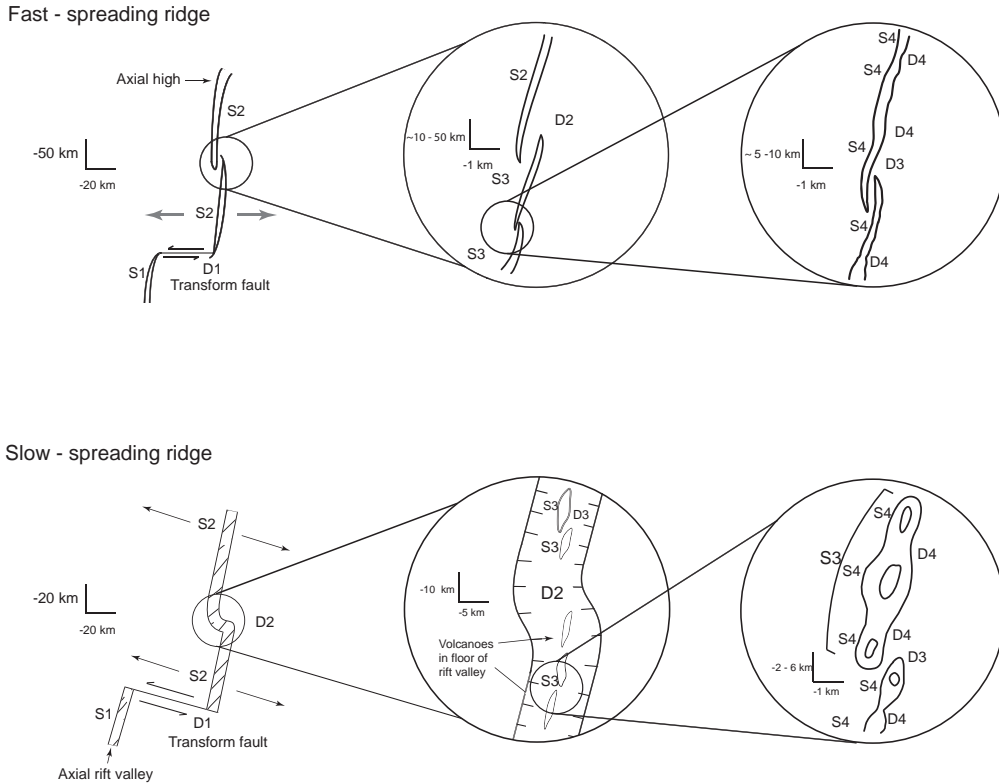


**Fig. 6.13** Summary of the hierarchy of segmentation on fast- and slow-spreading ridges.  $S_1$ ,  $S_2$ ,  $S_3$ , and  $S_4$  – first to fourth order ridge segments.  $D_1$ ,  $D_2$ ,  $D_3$ , and  $D_4$  – first to fourth order discontinuities (redrawn from Macdonald et al., 1991, *Science* **253**, 986–94, with permission from the AAAS).

The different scales and hence “orders” of ridge segmentation were first recognized on the fast-spreading East Pacific Rise. Segmentation also exists on the slow-spreading Mid-Atlantic Ridge but takes on somewhat different forms, presumably because the ridge crest is cooler and hence more brittle (Sempéré *et al.*, 1990; Gente *et al.*, 1995) (Fig. 6.13). First order segmentation is defined by transform faults, but overlapping spreading centers are absent and second order segments are bounded by oblique offsets of the ridge axis associated with deep depressions in the sea floor. Third and fourth order segmentation is in the form of geochemical variations and breaks in volcanic activity in the inner valley floor. The latter generate discrete linear volcanic ridges 2–20 km long and 1–4 km wide (Smith & Cann, 1993). Again first and second order segmentation is long-lived and third and fourth order segmentation is short-lived. Segmentation on the ultraslow-spreading Gakkel Ridge,

which does not even exhibit transform faulting, is in the form of volcanic and tectonic, or magmatic and amagmatic, segments (Michael *et al.*, 2003) (Section 6.9).

The first order segment boundaries, transform faults, are marked by pronounced bathymetric depressions (Section 6.12). They are often underlain by thinner crust than normal and anomalously low sub-Moho seismic velocities that may be due to partial serpentinization of the mantle as a result of seawater percolating down through the fractured crust. This thinning of the crust in the vicinity of fracture zones is particularly marked on the slow-spreading Mid-Atlantic Ridge (White *et al.*, 1984; Detrick *et al.*, 1993b). By contrast, the central portions of segments are elevated, have crust of normal thickness, and thinner lithosphere. This implies that the supply of magma from the mantle is focused at discrete points along the ridge axis at segment centers. These regions of thicker crust and enhanced



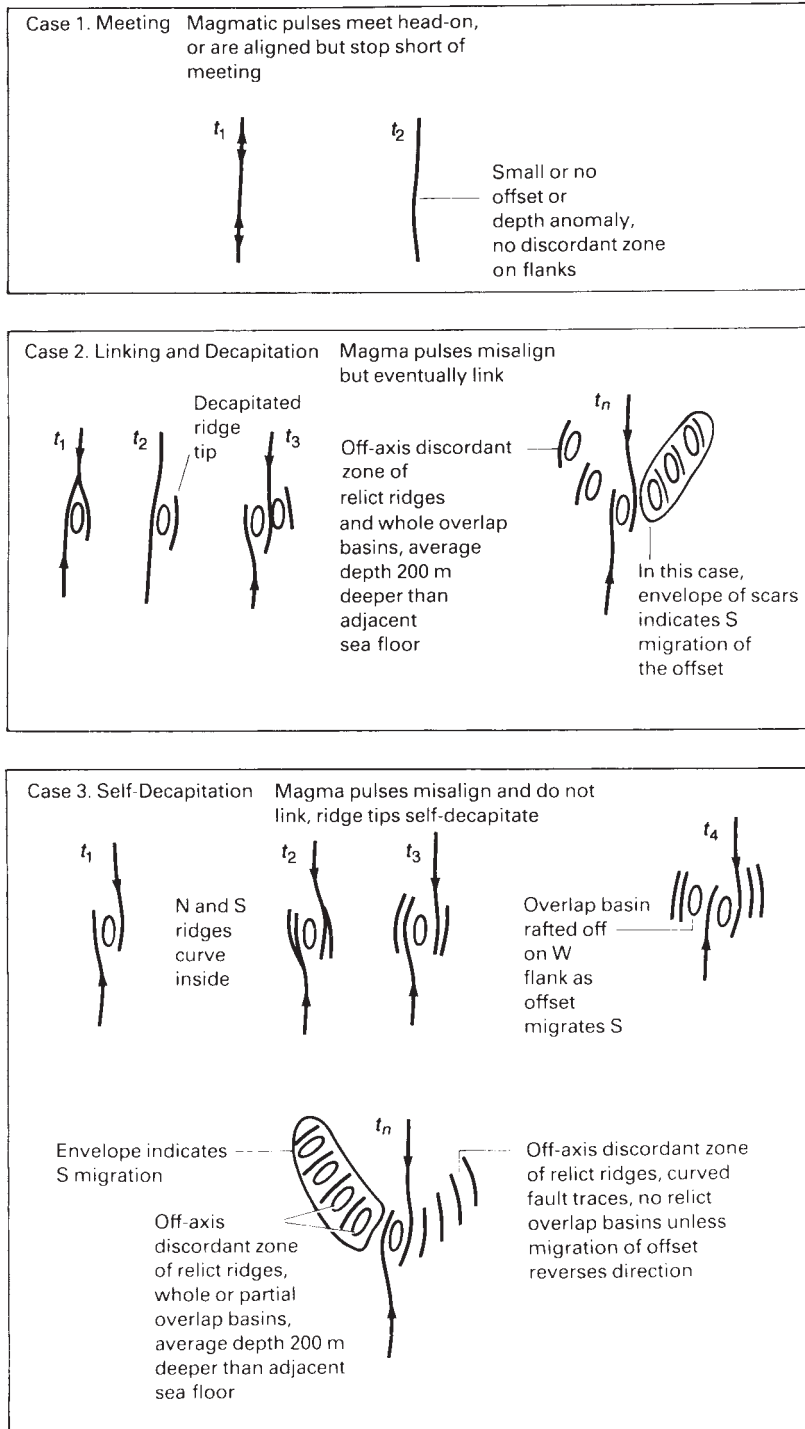


**Fig. 6.14** Three possible general cases for the evolution of ridge-axis discontinuities. Arrows along axis refer to direction of propagation of magmatic pulses.  $t_1, t_2, \dots, t_n$  refer to a time sequence. Cases 2 and 3 apply to second and third order discontinuities (after Macdonald et al., 1988, with permission from Nature **335**, 217–25. Copyright © 1988 Macmillan Publishers Ltd).

magma supply are characterized by negative mantle Bouguer anomalies (MBAs) and the areas of thinned crust between them by positive MBAs (Lin *et al.*, 1990). These latter areas include second order discontinuities in addition to transform faults. Evidence for the focusing of magma supply at segment centers is less obvious on the fast-spreading East Pacific Rise, but discontinuities and variations in the size and width of the magma chamber correlate with segmentation (Toomey *et al.*, 1990). These observations suggest that magma is emplaced at segment centers and migrates laterally along the ridge axis towards the segment ends. Increasingly it has been recognized that on cooler slow-spreading crust this can mean that segment ends are starved of magma and that parts of the crustal section consist of serpentinized mantle.

The extension of oceanic crust at ridge crests can occur either by the intrusion of magma or by extensional faulting. If ridge crests in the vicinity of transform faults are deprived of magma, amagmatic extension becomes more important. Perhaps the most spectacular expression of this is the occurrence of major low-angle detachment faults (Ranero & Reston, 1999; MacLeod *et al.*, 2002) (Section 7.3) on the inside corners of slow-spreading ridge–transform intersections that give rise to large corrugated and striated domes of serpentinized peridotite and gabbro (Plate 6.1 between pp. 244 and 245). These corrugated domes are exposed fault planes that deform the upper mantle and lower crust of oceanic lithosphere. The corrugations parallel the spreading direction and indicate the direction of motion on the fault. The offset on these faults is typically at least 10–15 km (Cann *et al.*, 1997). These exposures are thought to result from processes involving extension, detachment faulting, and crustal flexure that are similar to those that form metamorphic core complexes in zones of continental extension (Sections 7.3, 7.6.2, 7.7.3). For this reason the zones of exhumed peridotite at ridge–transform intersections are referred to as *oceanic core complexes*. Examples include the Atlantis Massif at the Mid-Atlantic Ridge–Atlantis transform intersection (Plate 6.1 between pp. 244 and 245) (Blackman *et al.*, 1998; Schroeder & John, 2004; Karson *et al.*, 2006) and along the Southeast Indian Ridge south of Australia (Baines *et al.*, 2003; Okino *et al.*, 2004).

Figure 6.15 illustrates the along axis variation of oceanic crust for slow- and fast-spreading ridges as envisioned by Cannat *et al.* (1995) and Sinton & Detrick (1992) respectively. Indeed Cannat *et al.* (1995) suggested

that serpentinized rocks may be much more common in the oceanic crust than previously assumed, even in areas distant from fracture zones. They dredged in the region of the North Atlantic Ridge at 22–24°N over areas of positive gravity anomalies, indicative of relatively thin crust, and over areas with a normal gravity field. Over the former, which comprised some 23% of the area surveyed, they encountered serpentinite with very few of the basaltic rocks which normally characterize oceanic layer 2. They suggested that as magmatic centers grow, migrate along the ridge axis and decline, the normal oceanic crust would similarly migrate and would enclose those regions of serpentinitic crust that originate where magma was absent. This work is important as it implies that serpentinized peridotite is more common in slow-spreading oceans than previously recognized. There are wide ranging implications. Peridotite is much more reactive with seawater than basalt and on weathering would release magnesium, nickel, chromium and noble metals. Serpentinite also contains far more water than altered basalt, which could account for much of the water supplied to the mantle in subduction zones (Section 9.8), although at the present day the only examples of oceanic crust formed at slow-spreading rates entering subduction zones are the Caribbean and Scotia arcs.

Segmentation of ocean ridges appears to be controlled by the distribution of partial melts beneath them (Toomey *et al.*, 1990; Gente *et al.*, 1995; Singh *et al.*, 1998), which feed magma chambers at discrete locations along them and create local depth anomalies. The ridge model of Sinton & Detrick (1992), described above, precludes extensive mixing within the small axial magma chamber along the ridge, and could explain the observed geochemical segmentation. With time the magma may migrate away from its sources, creating a gradual increase in depth of the axis as the pressure within it gradually wanes. This phenomenon may explain the noncoincidence of magma chamber and rise culmination noted by Mutter *et al.* (1988). The brittle shell overlying the magma stretches and cracks and magma intrudes so that eruptions follow the path of magma migration. After eruption the removal of supporting magma gives rise to the formation of an axial summit graben. Evidence for the pulse-like, episodic spreading of ridges, in which sea floor spreading occurs by fracturing, dike injection and copious volcanism, has been provided by seismological studies and direct observation (e.g. Dziak & Fox, 1999;

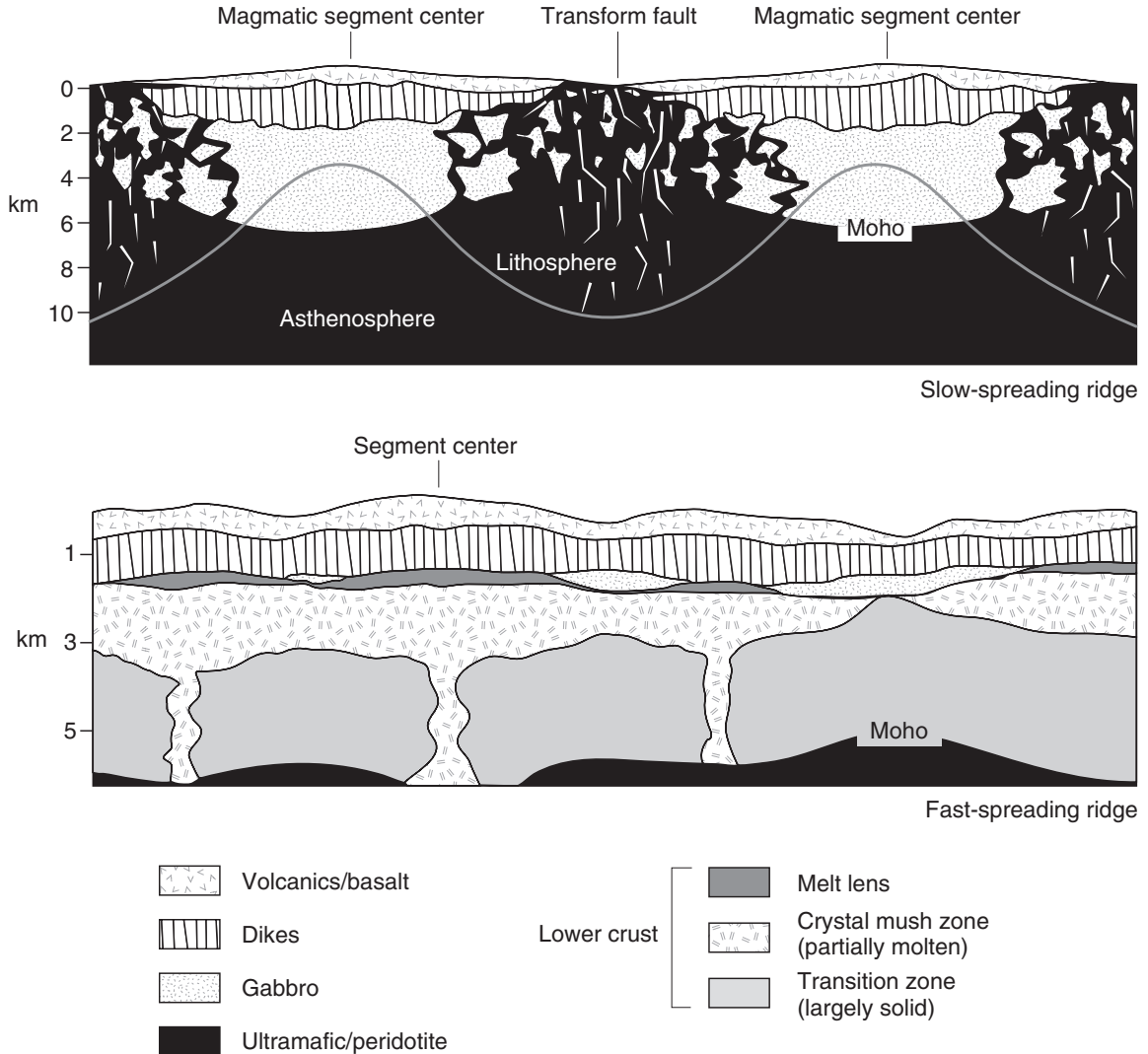


**Fig. 6.15** Along axis sections illustrating the variation in crustal structure between segment centers and segment ends on slow- and fast-spreading ridges, as envisioned by Cannat et al. (1995) and Sinton and Detrick (1992) respectively (redrawn from Cannat et al., 1995, with permission from the Geological Society of America, and modified from Sinton and Detrick, 1992, by permission of the American Geophysical Union. Copyright © 1992 American Geophysical Union).

Tolstoy *et al.*, 2001) and studies of ophiolites (Harper, 1978). Ridge axis discontinuities consequently occur where the magmatic pulses finally come to rest. The variable bathymetry and associated geophysical and

geochemical differences imply that adjacent segments of ridge have distinct, different sources in the mantle. First to third order segmentation is caused by the variable depth associated with magma migration; fourth

order effects are caused by the geochemical differences in magma supply.

## 6.8 PETROLOGY OF OCEAN RIDGES

Under normal conditions the peridotite of the upper mantle does not melt. However, the high heat flow at ocean ridges implies that the geothermal gradient crosses the peridotite solidus at a depth of about 50 km (Wyllie, 1981, 1988), giving rise to the parental magma of the oceanic crust (Fig. 2.36). A similarly high geothermal gradient is believed to exist beneath oceanic islands as oceanic lithosphere traverses a mantle plume or hotspot (Section 5.5), so generating basaltic rocks by a similar mechanism.

Mid-ocean ridge basalts (MORB) have the composition of olivine tholeiite (Kay *et al.*, 1970), and exhibit only minor variation in major element composition caused by variable alumina and iron contents. They may contain phenocrysts of olivine or plagioclase or, rarely, clinopyroxene (Nisbet & Fowler, 1978). The simplest interpretation of the chemistry of oceanic basalts, suggested from experimental petrology, is that separation of the partial melt occurs at a depth of 15–25 km. However, a wide range of alternative interpretations exist. The analysis of trace elements reveals that much of the compositional variation in the basalts is explicable in terms of high-level fractionation. To explain the most extreme variations, however, it is necessary to invoke the mixing of batches of magma. The frequent presence of xenocrysts of deep-level origin indicates that the rocks only spend a very short time in a high-level magma chamber.

On a smaller scale, a detailed sampling of the East Pacific Rise by Langmuir *et al.* (1986) revealed a series of basalts that are diverse in their major and trace element chemistry. This compositional variation has been interpreted in terms of a series of magmatic injection centers along the crest of the ridge which correlate with bathymetric highs spaced about 50–150 km apart. Magma moves outwards from the injection points along the ridge so that the temperature of eruption decreases regularly from maxima at the bathymetric

highs, which correspond to the centers of segments (Section 6.7). Batiza *et al.* (1988) sampled along the axis of the southern Mid-Atlantic Ridge, and showed that there are regular patterns of chemical variation along it caused by differences in the depth and extent of partial melting and degree of fractionation. They conclude that these patterns imply the presence of a deep central magma supply, with limited melt migration along the axis and no large, well-mixed magma chamber in the crust.

Flower (1981) has shown that differences in the lithology and chemistry of basalts generated at mid-ocean ridges show a simple correlation with spreading rate. The differences are not related to processes in the upper mantle, as the primary melts appear to be identical. They are believed to reflect the fractionation environment after partial melting. Slow-spreading systems are characterized by a complex magma chamber in which there is widespread accumulation of calcic plagioclase, the presence of phenocryst-liquid reaction morphologies, and pyroxene-dominated fractionation extracts. These phenomena are consistent with fractionation at many different pressures in a chamber that appears to be transient. This conclusion is in accord with the pattern of rare earth elements in basalts sampled from the Mid-Atlantic Ridge (Langmuir *et al.*, 1986). Although a homogeneous mantle source is suggested, the variations in rare earth chemistry apparent in samples from adjacent areas indicate a complex subsequent history of differentiation. Fast-spreading ridges, however, suggest low-pressure basalt fractionation trends to iron-rich compositions with little plagioclase accumulation or crystal-liquid interaction. This is consistent with the magma chamber being a stable and steady state feature.

Basalts from very slow- and ultraslow-spreading ridges have lower sodium and higher iron contents than typical MORB, reflecting a smaller degree of mantle melting and melting at greater depths. The geochemistry of the peridotites dredged from such ridges also indicates that the extent of mantle melting beneath the ridge is low. The great variation in the rate at which magma is supplied along the length of the Gakkell Ridge, and its lack of correlation with spreading rate, suggests that additional factors must be involved. Different thermal regimes or varying mantle composition along the length of the ridge, or lateral migration of melts in the upper mantle are some of the possibilities. Indeed, because of the smaller vertical

extent of melting beneath such ridges (Section 6.9), small variations in mantle temperature and/or composition would lead to greater proportional changes in the volume of magma produced (Michael *et al.*, 2003).

## 6.9 SHALLOW STRUCTURE OF THE AXIAL REGION

---

As noted above (Section 6.1), normal oceanic crust, that is, not formed in the vicinity of hot spots or transform faults, has a remarkably uniform seismic thickness of  $7 \pm 1$  km if generated at a full spreading rate in excess of  $20 \text{ mm a}^{-1}$ . For a homogeneous mantle this implies a comparable thermal gradient beneath all such ridge crests, and a similar degree of partial melting of the mantle, which produces the uniform thickness of mafic crust. The essential uniformity of the thermal regime beneath ridges is also implied by the lithospheric age versus depth relationship (Section 6.4). However, the rate at which magma is supplied to the crust will depend on the spreading rate. On fast-spreading ridges the magma supply rate is such that the whole crestal region at relatively shallow depth is kept hot and a steady state magma chamber exists. Indeed the crust above the magma chamber would be even hotter and weaker but for the cooling effect of hydrothermal circulation (Section 6.5). On slow-spreading ridges the lower rate of magma supply enables the crust to cool by conduction, as well as hydrothermal circulation, between injections of magma from the mantle. As a result the crust is cooler, and a steady state magma chamber cannot be maintained. At spreading rates of less than  $20 \text{ mm a}^{-1}$  this conductive cooling between injections of magma extends into the mantle and inhibits melt generation. This reduces the magma supply, as well as the magma supply rate, and hence the thickness of mafic crust produced, as observed on the Southwest Indian Ocean and Gakkel ridges (Section 6.1). It also makes the existence of even transient magma chambers beneath such ridges rather unlikely except beneath the volcanic centers (Section 6.6).

The relatively smooth axial topography of fast-spreading ridges is characterized by an axial high, up to 400 m in height and 1–2 km wide, and fault scarps with a relief of tens of meters, the fault planes dipping either towards or away from the ridge axis. Active volcanism is largely confined to the axial high, and the smooth topography is thought to result from the high eruption rate and the low viscosity of the magma. The axial high appears to correspond to and to be supported by the buoyancy of the axial magma chamber beneath. Studies of major fault scarps and drill core from DSDP/ODP drill hole 504B, all in Pacific crust, reveal that at depth the lava flows dip towards the ridge axis at which they were erupted and that the dikes beneath them dip away from the ridge axis (Karson, 2002). This geometry indicates a very narrow and persistent zone of dike intrusion, and isostatic subsidence as the thickness of the lava flow unit increases away from the point of extrusion (Section 6.10). This relatively simple structure of the upper crust at the crests of fast-spreading ridges is illustrated in Fig. 6.16.

The shallow structure at the crests of slow-spreading ridges is fundamentally different to that on fast-spreading ridges (Smith & Cann, 1993). As a result of less frequent eruptions of magma and a cooler, more brittle upper crust, extension by normal faulting is more pronounced. The fault scarps have approximately 100 m of relief and the fault planes dip towards the ridge axis. Volcanism is essentially confined to the inner valley floor, and at any one time appears to be focused along specific axis-parallel fissures, forming axial volcanic ridges 1–5 km wide and tens of kilometers in length. As these ridges move off axis, as a result of further accretion, they may be cut by the faults that ultimately form the bounding scarps of the median valley. The spacing of these bounding faults appears to be about one-third to one-half of the width of the inner valley, that is, several kilometers. Within the inner valley floor the topography is fissured and cut by small throw normal faults, the density of these features giving an indication of its age. There is clear evidence of alternate phases of volcanic and tectonic (magmatic and amagmatic) extension of the crust, as one would expect if there are transient magma chambers beneath, which supply discrete packets of magma to the inner valley floor.

Very slow-spreading ridges are characterized by thin mafic crust and large regions of peridotite exposures where the mantle appears to have been emplaced directly to the sea floor. However there are also magmatic segments analogous to the second order

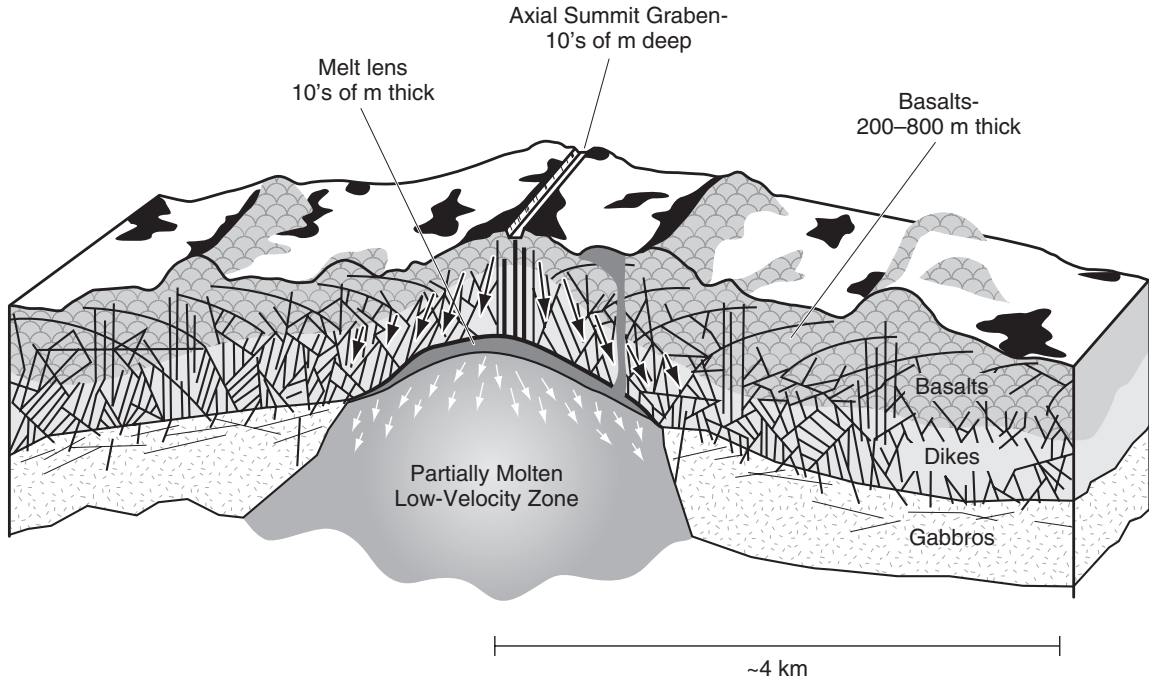


**Fig. 6.16** Schematic diagram of the upper crustal structure for a fast-spreading ridge (redrawn with permission from Karson, *et al.*, 2002 by permission of the American Geophysical Union. Copyright © 2002, American Geophysical Union).

segments on slow-spreading ridges. These have abundant volcanoes, typically in the form of axial volcanic ridges. These are 15–25 km long, and rise 400–1500 m from the axial valley floor. In the amagmatic sections the rift valley is often deeper than on slow-spreading ridges, up to 5000 m deep in places, and the rift valley walls have up to 2000 m of relief. On the Gakkel Ridge the western section is magmatic, the central section essentially amagmatic, less than 20% of the rift valley having a basaltic cover, and the ultraslow-spreading eastern section is very different again. It has six large volcanic centers on it that extend for 15–50 km along axis and are 50–160 km apart. These volcanic edifices are larger and more circular than those on other ridges. The amplitudes of the magnetic anomalies recorded between the volcanic centers suggest that the basaltic cover is thin in these tectonized zones. These marked along-axis contrasts in the extent of magma supply, which do not correlate with spreading rate, pose interesting questions regarding the generation and/or migration of melts beneath the ridge (Section 6.8) (Michael *et al.*, 2003).

## 6.10 ORIGIN OF THE OCEANIC CRUST

A widely accepted model of the petrologic processes occurring at ocean ridges was proposed by Cann (1970, 1974). In this model hot asthenospheric material ascends buoyantly (Nicolas *et al.*, 1994) sufficiently rapidly up a narrow zone to pass through the basalt melting curve and provides an interstitial melt of basaltic composition. The molten fraction increases in volume as the asthenosphere rises, and eventually departs the parental material to ascend independently and produce a magma chamber within the lower part of the oceanic crust at the level of layer 3. Part of this magma rises through fissures in the crust and erupts onto the ocean floor to produce pillowed lava flows. Beneath the flows is a zone of dikes formed by solidification of magma in the fissures that feed the flows. The lavas and dikes together make up layer 2 of the oceanic crust. Kidd (1977)

modeled these processes of extrusion and intrusion and compared them with observations of ophiolite complexes. Layer 2C was found to consist entirely of sheeted dikes, which were intruded through zones less than 50 m wide. The dikes show some 10% more chilled margins on one side than the other, showing that approximately 10% of the dikes are cut by later dikes, such that the margins of the original dikes ended up on opposite sides of the ridge crest. The symmetry of sea floor spreading about the ridge axis is explained because dike intrusion will proceed preferentially into the hot central axis where existing dikes are weakest. It was suggested that the lavas extruded above the dikes cool rapidly in contact with sea water and flow less than 2 km before solidification. Lavas and dikes are predicted to rotate towards the ridge crest as they move away from the zone of extrusion as a result of isostatic adjustment (Fig. 6.17). They also undergo metamorphism near the ridge axis as they equilibrate at high temperatures in the presence of seawater.

This model for the origin of layer 2 has received striking confirmation from studies of sections through the upper crust revealed by major fault scarps and drill core from DSDP/ODP drill hole 504B, all in fast-spreading Pacific crust (Karson, 2002) (Section 6.9). Furthermore the model predicts that beneath the axial high the extrusive layer should be very thin and the dikes correspondingly closer to the sea floor (Fig. 6.17). This is confirmed by seismic studies that reveal a narrow central band of high seismic velocities beneath the axial high (Toomey *et al.*, 1990; Caress *et al.*, 1992) and a thin extrusive layer that thickens rapidly off axis within 1–2 km (Detrick *et al.*, 1993b; Kent *et al.*, 1994).

In the model of Cann (1974) the crust at lower levels develops from the crystallization of the axial magma chamber. The first minerals to crystallize in the magma chamber, olivine and chrome spinel, fall through the magma and form a basal layer of dunite with occasional accumulations of chromite. With further cooling pyroxene crystallizes and cumulate peridotitic layers (i.e. of olivine and pyroxene) are produced, giving way upwards to pyroxenites as the crystallization of pyroxene begins to dominate. Ultimately, plagioclase also crystallizes and layered olivine gabbros form. Much of the residual liquid, still volumetrically quite large, then solidifies over a very small temperature range to form an upper, “isotropic” gabbro. A small volatile-rich residuum of this differentiation process, consisting essentially of plagioclase and quartz, is the last fraction to crystallize, sometimes intruding upwards to form veins and small

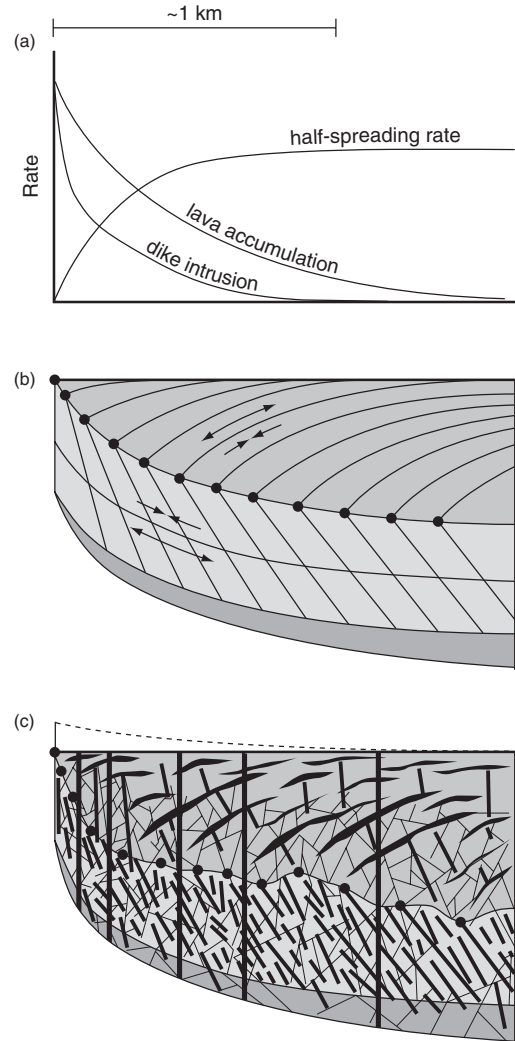


**Fig. 6.17** Geologic interpretation of the model of Kidd (1977) for the construction of Layer 2 at a fast-spreading ridge crest. Note the prediction of a rapid increase in the thickness of the extrusive layer away from the ridge axis and the presence of dikes at shallow depths near the ridge axis (redrawn with permission from Karson, *et al.*, 2002, by permission of the American Geophysical Union. Copyright © 2002 American Geophysical Union).

pockets of “plagiogranite” within the overlying sheeted dike complex. The abundance of volatiles, notably water, in the uppermost part of the magma chamber may be due, at least in part, to interaction with seawater percolating downwards and/or stoping of the

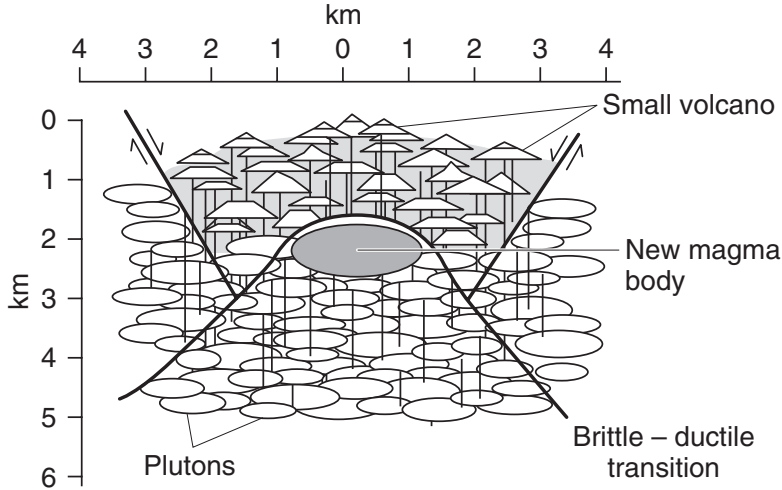


**Fig. 6.18** Model for the construction of oceanic crust at a slow-spreading ridge. Transient magma bodies rise to the brittle–ductile transition within the crust and shoulder aside and depress older plutons. Part of the magma body erupts through a fissure to produce a volcano or hummocky lava flow on the sea floor and the remainder solidifies to form part of the main crustal layer (redrawn from Smith & Cann, 1993, with permission from *Nature* **365**, 707–15. Copyright © 1993 Macmillan Publishers Ltd).

overlying, hydrothermally altered dikes into the magma chamber.

The two gabbro units, isotropic and layered, are often correlated with seismic layers 3A and 3B, respectively (Section 2.4.7). The ultramafic cumulates, rich in olivine and pyroxene, would then account for the sub-Moho seismic velocities. Thus, the Moho occurs within the crystallized magma chamber at the base of the mafic section. Off axis, however, in a lower temperature environment, the uppermost ultramafics may become partially hydrated (i.e. serpentinized) and as a result acquire lower seismic velocities more characteristic of layer 3B. The seismic Moho would then occur at a somewhat greater depth, within the ultramafic section. As a result of this uncertainty in defining the seismic Moho, petrologists have tended to define the base of the crust as the base of the presumed magma chamber, that is, the dunite/chromitite horizon. Hence, this level is termed the “petrologic Moho”.

The model of Cann (1974) and Kidd (1977) has met with considerable success in explaining the known structure and petrology of oceanic crust created at fast-spreading ridge crests, where there is a steady state magma chamber. At slow-spreading ridge crests, however, the zone of crustal accretion is wider and it seems probable that magma chambers are only tran-

sient. In this case the alternative model derived from early reinterpretations of ophiolites in terms of sea floor spreading may be more applicable. This invoked multiple small magma chambers within the main crustal layer in the light of the multiple intrusive relationships observed at all levels in the Troodos ophiolite of southern Cyprus (Moores & Vine, 1971) (Section 2.5). Smith & Cann (1993) favor such a model for the creation of oceanic crust at slow-spreading ridge crests (Fig. 6.18). However away from segment centers, and particularly in the vicinity of transform faults, the magma supply may be greatly reduced, and serpentinized mantle peridotite appears to be a common constituent of the thinned oceanic crust. This type of crust becomes even more common on very slow-spreading ridges and ultimately most of the crust is effectively exposed mantle with or without a thin carapace of basalts. On the ultra-slow Gakkel Ridge the crust is essentially serpentinized and highly tectonized mantle peridotite with volcanic centers at intervals of  $100 \times 50$  km.

An alternative approach to understanding the accretionary processes at mid-ocean ridge crests is by way of thermal modeling (Sleep, 1975; Kuszniir & Bott, 1976; Chen & Morgan, 1990). Chen & Morgan (1990) made significant improvements to such models by including the effects of hydrothermal circulation at ridge crests



and the different rheological properties of the crust compared to the mantle, oceanic crust being more ductile at high temperatures than the mantle. As outlined in Section 6.9, the thermal regime beneath a ridge crest is influenced by the rate at which magma is supplied to the crust, which depends on the spreading rate. As a consequence the brittle–ductile transition (at approximately 750°C) occurs at a shallower depth in the crust at a fast-spreading ridge compared to a slow-spreading ridge that has a lower rate of magma supply. This in turn implies that at a fast-spreading ridge there is a much greater volume, and hence width, of ductile lower crust. This ductile crust effectively decouples the overlying brittle crust from the viscous drag of the connecting mantle beneath, and the tensile stresses pulling the plates apart are concentrated in a relatively thin and weak layer that extends by repeated tensile fracture in a very narrow zone at the ridge axis. On a slow-spreading ridge the brittle layer is thicker and the volume of ductile crust much smaller. As a result the tensile stresses are distributed over a larger area and there is more viscous drag on the brittle crust. In this situation the upper brittle layer deforms by steady state attenuation or “necking” in the form of a large number of normal faults creating a median valley.

Chen & Morgan (1990) demonstrated that for crust of normal thickness and appropriate model parameters the transition from smooth topography with a buoyant axial high to a median rift valley is quite abrupt, at a full spreading rate of approximately 70 mm a<sup>-1</sup> as observed. The model also predicts that for thicker crust forming at a slow rate of spreading, as for example on the Reykjanes Ridge immediately south of Iceland, there will be a much larger volume of ductile crust, and smooth topography is developed rather than a rift valley. Conversely, where the crust is thin on a slow-spreading ridge, for example in the vicinity of fracture zones on the Mid-Atlantic Ridge, the median valley will be more pronounced than at a segment center. Such instances of thicker or thinner crust than normal are also likely to be areas of higher or lower than normal upper mantle temperatures respectively which will enhance the effect in each case. The model was extended by Morgan & Chen (1993) to incorporate a magma chamber as observed on the East Pacific Rise. This enhanced model predicts that a steady state magma chamber can only exist at spreading rates greater than 50 mm a<sup>-1</sup> and that the depth to the top of the chamber will decrease as spreading rate increases, whilst retaining the essential features of the Chen & Morgan (1990) model.

In general therefore there is good agreement between the theoretical models for the creation of oceanic crust and observations made on *in situ* ocean floor and on ophiolites. Certain aspects however are still problematic. The evolution of a median valley as accretion occurs, that is, the way in which its flanks are uplifted and the normal faults ultimately reversed, is poorly understood. This is particularly true for the amagmatic segments of very slow- and ultraslow-spreading ridges where mantle material is emplaced directly to the sea floor. The details of the formation of the gabbroic layer 3, from a steady state or transient magma chamber, are also the subject of much debate.

## 6.11 PROPAGATING RIFTS AND MICROPLATES

---

The direction of spreading at an ocean ridge does not always remain constant over long periods of time, but may undergo several small changes. Menard & Atwater (1968) proposed that spreading in the northeastern Pacific had changed direction five times on the basis of changes in the orientation of major transform faults (Section 5.9) and magnetic anomaly patterns. Small changes in spreading direction have also been proposed as an explanation of the anomalous topography associated with oceanic fracture zones (Section 6.12).

Menard & Atwater (1968) made the assumption that the reorientation of a ridge would take place by smooth, continuous rotations of individual ridge segments until they became orthogonal to the new spreading direction (Fig. 6.19a). The ridge would then lie at an angle to the original magnetic anomaly pattern. Long portions of ridges affected in this way might be expected to devolve into shorter lengths, facilitating ridge rotation and creating new transform faults (Fig. 6.19b). The change in spreading direction is thus envisaged as a gradual, continuous rotation that produces a fan-like pattern of magnetic anomalies that vary in width according to position.

An alternative model of changes in spreading direction envisions the creation of a new spreading center